The Impact of Surface Voltage on Photoluminescence Response for the Detection of Copper and Iron Contamination in Silicon

Thomas Nassiet,* Romain Duru, Delphine Le-Cunff, Georges Bremond, and Jean-Marie Bluet

Herein, silicon substrates intentionally contaminated by iron and copper are analyzed by an innovative technique based on photoluminescence (PL) measurement, with the aim to evaluate the sensitivity of this technique to low level contamination and its capability for further in-line monitoring during devices fabrication. Measurements are carried out directly after samples preparation, with the combined use of PL and corona discharges to separate the contribution of metallic contamination from interface properties on the PL signal. The sensitivity of PL to both iron and copper contamination in silicon with higher sensitivity when surface recombination is minimized is shown. Therefore, this work highlights the importance of surface properties monitoring for the optimization of PL detection of metallic contamination.

1. Introduction

With the development of imaging technologies, the detection of low-level metallic contamination has become a compulsory research area to control the reliability and performance of devices.[1,2] Early detection of unexpected metallic contaminants during device fabrication is key to avoid yield losses and secure the manufacturing line.[3,4] However, most of the techniques used to detect contamination share at least one of the major problems: the detection limit of the technique is too high (e.g., EDX); the technique is only sensitive to surface (e.g., TXRF) or volume (e.g., SPV).[5–7] Some techniques are also invasive and requires the destruction of the wafer after the measurement, without being able to reintegrate into the production line (e.g., TOF-SIMS, ICP-MS).[8,9]

Among the existing techniques to characterize metallic contamination in silicon, room temperature photoluminescence (PL) performed in an industrial environment is explored in a very specific way as a noncontact and noninvasive alternative for the detection of low-level metallic contamination. PL is highly sensitive to electrically active defects in the Si crystal at various depths depending, among other parameters, on the selected excitation wavelength and has been studied for its capability to detect and monitor metallic contamination.[10–12] However, it is well known that PL is also sensitive to surface states and related recombination.[13] Therefore, it is important to find a method to decorrelate these two phenomenon and avoid wrong interpretation.

In our approach, we rely on local corona charging to control the surface potential of the wafer and surface recombination velocity, combined with a Kelvin probe for contactless reading of the resulting voltage.[14] To demonstrate the potential of this method, PL measurements have been carried out on intentionally contaminated Si wafers with iron and copper. Results before and after surface potential modification are presented and discussed based on known recombination processes in both Si surface and volume.

2. Experimental Section

2.1. Sample Preparation

Samples were prepared from boron doped (100) oriented 300 mm CZ Si wafers with doping concentrations between $N_A = 9.0 \times 10^{14}$ and 1.7×10^{15} cm^{-3}. After HF surface cleaning, iron and copper ionic solutions were spin coated on the wafers at four different concentrations from 10^{10} to 10^{13} cm^{-2}, controlled by TXRF. Samples were then annealed at 750 °C during 300 s under an O_2 saturated atmosphere to generate between 8.6 and 9.2 nm thick Si oxide on both front and rear surfaces, measured by ellipsometry and depending on nucleation rate.[15] Dummy wafers were also used to avoid metallic cross-contamination during annealing. Finally, two uncontaminated reference samples were generated without and with the anneal (respectively Ref#1 and Ref#2) for a proper comparison to

T. Nassiet, R. Duru, D. Le-Cunff
Metrology
STMicroelectronics
850 Rue Jean Monnet, 38920 Crolles, France
E-mail: thomas.nassiet1@st.com

G. Bremond, J.-M. Bluet
CNRS
INSA Lyon
Institut des Nanotechnologies de Lyon (INL)
Université de Lyon
UMR-5270, 69100 Villeurbanne, France

contaminated samples and to show the impact of the contamination process and the presence of a passivation layer on the PL signal.

2.2. Photoluminescence Measurement

Photoluminescence measurement is a two-steps process involving, at first, the absorption of a photon by the Si substrate and the associated generation of an electron–hole pair. In a second time, the electron will recombine with a hole, following several available processes,[13] directly from the conduction band to the valence band, or using energy levels formed by crystalline defects or contamination. The carrier recombination can be radiative or nonradiative, depending on the occurring process: at low irradiance levels (concentration of generated electron–hole pairs lower than substrate doping), recombinations are dominated by radiative and Shockley–Read–Hall (SRH) processes. At high irradiance (concentration of generated electron–hole pairs higher than substrate doping), auger recombinations appear no more negligible and tend to dominate all processes as the irradiance grows higher. In samples where defect level density is important in the Si gap, a combined effect of SRH and Auger mentioned as trap assisted auger (TAA) can also occur and become as impactful as basic auger.[16]

Full wafer PL image (MacroPL) was acquired with a PL imaging industrial equipment by scanning the samples with a 808 nm laser excitation and an irradiance of 7.6×10^{20} photons s^{-1} cm^{-2}. The PL signal was locally integrated from 800 to 1600 nm using a 2D array InGaAs camera. PL spectroscopy (PLS) was also performed with another equipment to extract PL spectra using a 638 nm laser excitation with an irradiance of 2.4×10^{21} photons s^{-1} cm^{-2} and a spectrometer equipped with an InGaAs photodetector. The penetration depth is respectively of few micrometers at 638 nm excitation and a dozen of micrometers for 808 nm (**Figure 1**). Moreover, the depth of field for MacroPL measurement contains all wafer thickness, making the later more sensitive to volume properties contrary to PLS that is essentially sensitive to surface effects. Both MacroPL and PLS selected irradiances have been shown to generate more electron–hole pair than the initial sample doping. Thus, both PL measurements were performed under high excitation density and all recombination processes must be considered to explain the signal behavior.
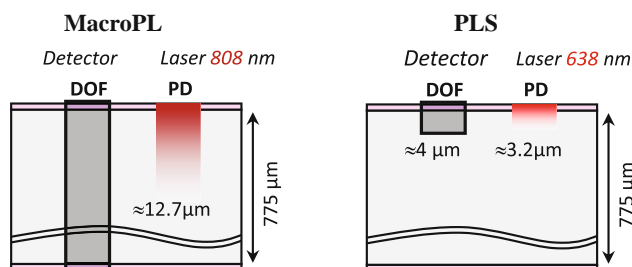
2.3. Complementary Techniques

2.3.1. Contamination Analysis

The concentration of both metallic contaminants was monitored thanks to total reflection X-ray fluorescence (TXRF) before the annealing process. TXRF is a surface measurement technique, thus the Si oxide layer highly reduces the sensitivity of TXRF to the Si/SiO$_2$ interface and additional technique such as secondary ion mass spectroscopy (SIMS) was needed instead to monitor contamination after annealing. SIMS profiles obtained for the two most contaminated samples after annealing are presented in **Figure 2**. These profiles are representative of all samples and show that both iron and copper contamination are essentially accumulated in the first 50 nm of the wafer. This is coherent with a 750 °C thermal budget with slow sample cooling for iron and copper contamination in Si. More deeply, detection limit of those metallic elements with SIMS is reached. Therefore, only quantitative surface contamination concentrations can be extracted from SIMS measurements.

In boron doped Si substrates contaminated with iron, both iron and boron atoms can interact with each other by forming electrostatic bonds. The required energy to break these bonds is moderate and such "activation" can be performed with a high photon excitation. Iron–boron pairs and interstitial iron do not share the same electrical behavior in Si. Therefore, measuring carrier lifetime before and after iron–boron pairs activation enables the determination of the density of iron atoms in the Si volume. This behavior is the main principle behind quantitative volume iron determination using surface photo-voltage (SPV), where iron activation reduces carrier measured lifetime.[17] During the PL processes, the samples are repeatedly excited with high photon excitation. Consequently, we consider that most of the iron is activated and the measured PL variations are associated to interstitial iron behavior. This has been demonstrated following experiments that are not presented in this work.
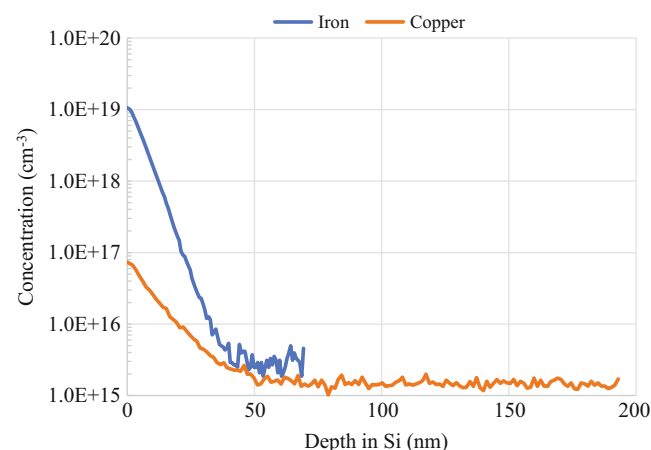

Figure 1. Schematic of the depth of field (DOF) for the MacroPL and PLS techniques and their respective laser penetration depth (PD).

Figure 2. SIMS profiles of the two iron and copper most contaminated samples.

2.3.2. Surface and Interface Properties

Contactless quasi-static capacitance–voltage measurement was performed using corona oxide characterization of semiconductors (COCOS) technique where surface potential is measured with a vibrating Kelvin probe and adjusted using corona discharges.[18] By measuring surface potential in dark conditions and under high irradiance (**Figure 3**), surface barrier "V_{sb}" can be extracted and inform about the samples band regime. By convention for p-doped Si, V_{sb} is positive when the bands are bent downward. The samples are then positioned into the accumulation regime when $V_{sb} < 0$, in depletion when $0 < V_{sb} < \Delta E_F$ and in inversion when $V_{sb} > \Delta E_F$. ΔE_F corresponds to the drift of the Fermi level due to the initial samples doping; in our case, $\Delta E_F \approx 0.3$ V.

As COCOS is based on quasi-static C–V measurement, it was also used to extract samples main passivation parameters: interface defect density (D_{it}) and total charges in the silicon oxide (Q_{tot}). These passivation parameters will appear to be essential to understand the impact of the contamination on the PL signal.

2.3.3. Bias Dependent Photoluminescence

By combining PLS measurement from a first industrial equipment, and corona discharges and surface potential measurement from a second one, it is possible to plot bias dependent photoluminescence (PL–V) curves with band regime going from accumulation to strong inversion though depletion.[14] This technique has been acknowledged by its similarity to capacitance–voltage measurement and its sensitivity to interface quality.

Figure 4 shows an example of PL–V measurement obtained on the noncontaminated Ref#2 sample. The PL signal is strongly dependent on the band regime and can drop by 90% going from accumulation to the onset of inversion. Therefore, knowing the samples band regime is essential for parameters discretization when studying PL signal.

3. Results and Discussion

3.1. Initial Measurements

In this paragraph, we discuss about the initial PL measurements performed after the anneal and before any surface modification. As previously explained in our experimental setup, MacroPL and PLS are two complementary techniques: the first one is more sensitive to volume parameters and enables full wafer images while the second one is more sensitive to surface behavior. Therefore, spatially localized effects will be more easily identified with MacroPL.

Figure 5 shows full wafer PL images of reference sample Ref#2, and the two most contaminated wafers respectively with copper and iron. On Ref#2 image, some small dark spots are visible. Thanks to SPV measurement, these spots were directly associated to very low iron contamination ($< 3 \times 10^{10}$ cm^{-3}), brought on the wafer during samples handling. By measuring

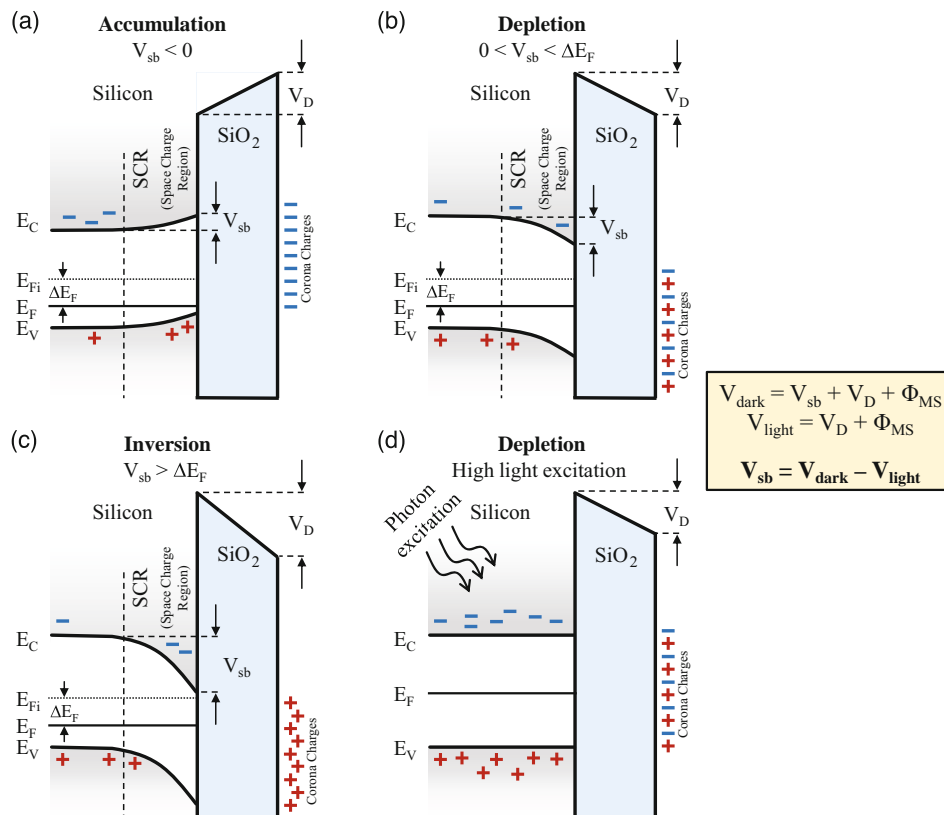**Figure 3.** Band diagram of a p-Si/SiO$_2$ interface in a) accumulation, b) depletion, c) inversion, and d) in depletion under high light excitation.
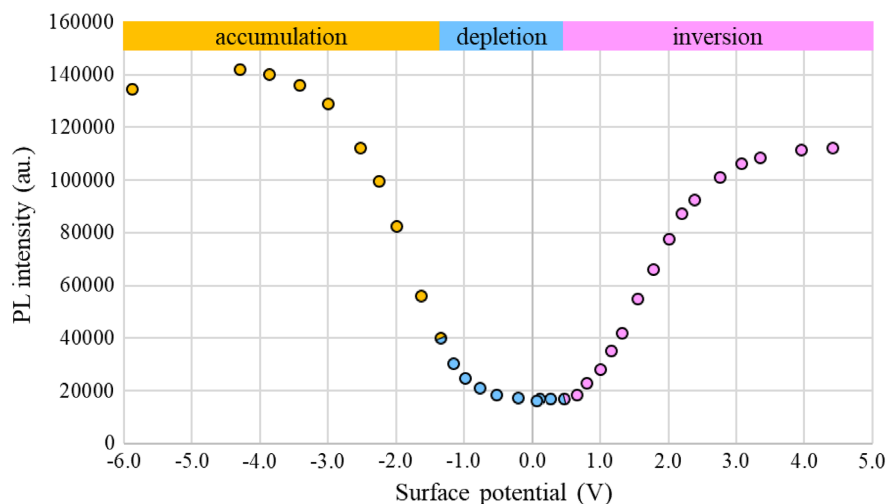
Figure 4. PL-V measurement of noncontaminated sample ref. [2] and description of band regime.
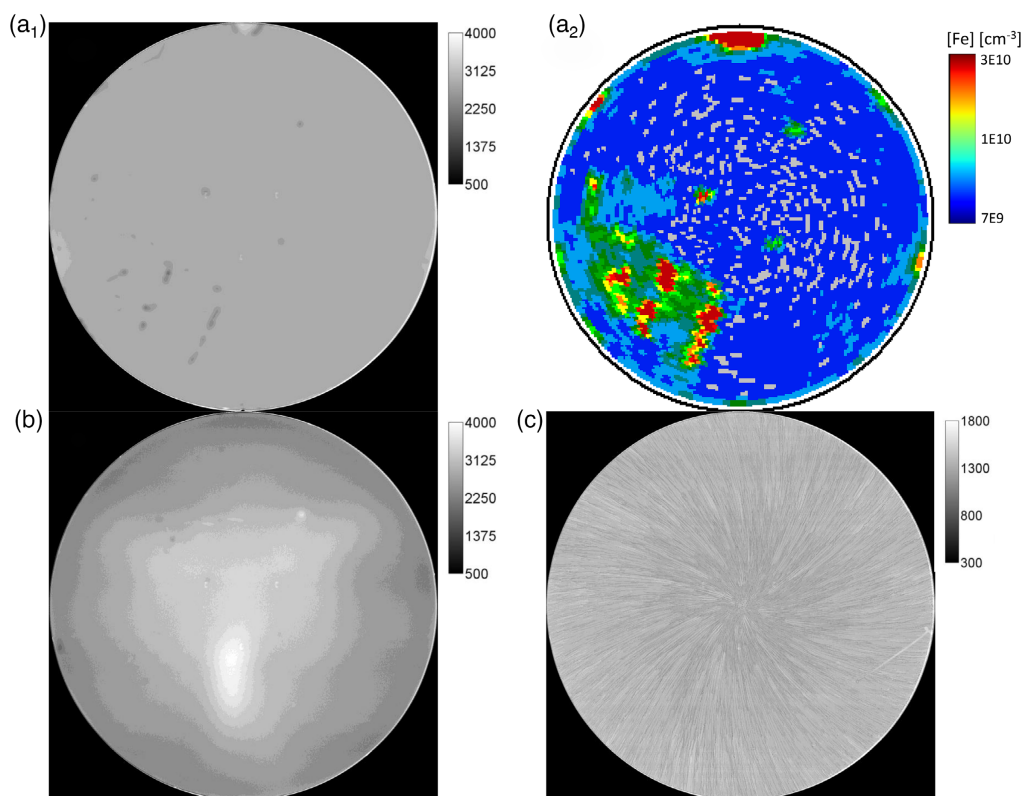

Figure 5. MacroPL measurement of ref. [2] (a_1), associated SPV iron mapping (a_2) and MacroPL of the most contaminated wafer with copper (b) and iron (c).

average PL intensity on the entire wafer, we can then neglect the contribution of those small involuntary contaminated areas. During PLS measurement we also paid attention to select measurement sites far from those contaminated areas.

Copper contaminated sample shows some brighter areas with erratic position not correlated to deposition process, contrary to iron that clearly displays a spin coating signature. At 750 °C

during 5 h, diffusion length of both iron and copper are larger than the wafers thicknesses. Differences between diffusivity of both contaminants can then be neglected. However, iron solubility in Si is equal to $C_{Si}(Fe) = 6.0 \times 10^{11}$ cm^{-3} while it is five order of magnitude higher for copper: $C_{Si}(Cu) = 2.5 \times 10^{16}$ cm^{-3}.[2] Therefore, all the deposited iron at the wafer surface cannot enter into the Si crystal and

inhomogeneous deposition during spin coating is still visible after the anneal.

Figure 6 draws a comparison between post-anneal MacroPL intensity and PLS measurement in function of initial TXRF contamination measurement. Before considering the contaminated samples, a first observation to be made is the increase of PL between Ref#1 and Ref#2. This strong increase is only associated to SiO_2 surface passivation and the reduction of surface recombination velocity. This highlights not only the interest of surface passivation to increase PL signal, but also show that equivalent surface passivation condition is necessary to compare samples.

Copper contaminated wafers show a counterintuitive behavior on both PL measurements with a first increase of PL at surface concentration 3×10^{12} cm^{-2}, followed by the expected decrease of signal due to electrical activity of copper centers in Si. This behavior has been discussed before and it has been explained by an interface defect reduction from the interaction of copper atoms with surface states.[19] Indeed, from COCOS, a decrease of interface states density has been measured for the corresponding sample (Table 1), corroborating previous hypothesis. However, until PL–V measurement presented later, reduction of D_{it} cannot yet justify on its own the increase of PL, as other passivation parameters can also lead to a signal increase.

Iron contaminated wafers act differently between PLS and MacroPL measurement, highlighting a possible difference between surface and volume behaviors. PLS shows only a decrease of PL with increasing contamination while MacroPL intensity unexpectedly fluctuates. As mentioned before, the
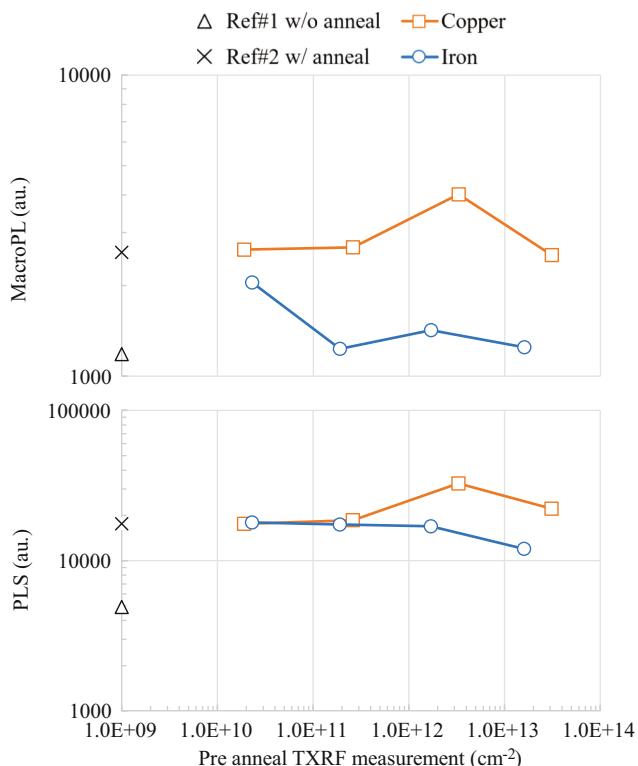
Table 1. Pre-anneal concentration from TXRF, post-anneal surface concentration from SIMS, volume iron concentration from SPV, and interface defect density D_{it} values obtained from COCOS measurement.

	Initial concentration TXRF [cm^{-2}]	Final concentration SIMS [cm^{-3}]	SPV [Fe] [cm^{-3}]	D_{it} [eV cm^{-2}]
Ref#2				1.45E12
Copper	1.9E10	1.8E16		1.33E12
	2.6E11	3.0E16		1.28E12
	3.3E12	5.2E16		1.06E12
	3.1E13	7.8E16		1.15E12
Iron	2.3E10	9.0E15	3.74E11	1.41E12
	1.9E11	1.3E17	2.60E12	1.40E12
	1.7E12	2.6E18	1.24E12	1.36E12
	1.6E13	1.0E19	8.93E11	1.42E12

solubility limit for iron in Si at 750 °C is not sufficient to enable all deposited contamination to enter the crystal. Therefore, a major quantity of iron have remained close to the surface as showed on SIMS profile. Still, iron surface contamination measured with SIMS do not correlate with SPV measurement variations. This can also be explained by the previously mentioned solubility of iron in Si and by the fact that SPV technique is considered to be intrinsically unsensitive to the first 10 µm of the crystal during measurement. As the iron atoms are predominantly present at the near surface, difference in reading can be anticipated.

It is to be pointed out that all the previously described PL fluctuations do not consider surface band regimes and associated samples initial passivation status. To associate PL variation to the presence of metallic contamination, it is necessary to remove surface charging effects.

3.2. PL–V Measurements

To overcome very low surface potential fluctuation due to unidentical interface passivation quality during the annealing process, all samples were measured with PL–V technique. In this section, PL–V curves are discussed and compared as a function of measured SIMS surface contamination, with the main goal to differentiate between PL variations due to surface properties and metallic contamination effects.

3.2.1. Iron

Figure 7 shows the PL–V curves obtained for the iron contaminated samples. All iron wafers were initially found in depletion. Thus, in this band regime, PL intensity and its variations are identical to Figure 6 and only the PL intensity drop of the most contaminated sample is noticeable among all wafers. In both accumulation and inversion regimes, PL–V variations as a function of contamination are much more significant than in depletion. The PL–V variations in all band regimes are consistent with SIMS post-anneal measurements, but not with SPV. This behavior is certainly due to the solubility mechanism previously
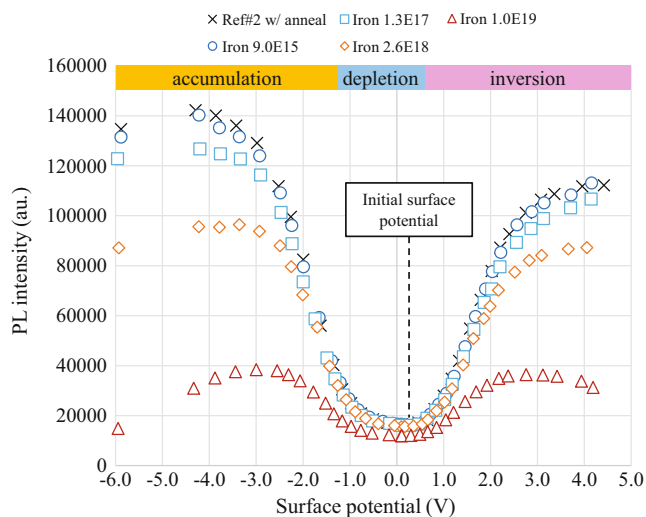

Figure 6. Initial MacroPL and SPL measurements of all samples after annealing (no surface modification) in function of pre-anneal TXRF concentration measurements.

Figure 7. PL–V measurement of iron samples as a function of post-anneal SIMS surface concentration measurement [cm^{-3}].

Figure 8. PL–V measurement of copper samples as a function of post-anneal SIMS surface concentration measurement [cm^{-3}].

explained and the low diffusivity of iron in Si that accumulates in the volume close to the surface.

In accumulation, the electric field generated by the corona charges passivates the surface and minimizes possible surface recombination with interface states because most of the electrons have diffused toward the volume.[20] The electron–hole pairs generated during the PL process are free to recombine in the Si volume and the recombination probability with potential defect levels due to iron contamination becomes the highest. In term of recombination processes, the surface SRH is minimized, and the PL signal is then more sensitive to the volume SRH and TAA that both depend on defect level density in the Si bandgap. All iron contaminated wafers show then a PL intensity decrease that follows the contamination level, with a 90% drop for the most contaminated sample compared to the reference.

Contrary to accumulation, depletion regime enhances surface recombination as most of the generated electrons are driven to the surface. Surface recombination becomes dominant over volume SRH and TAA, and strongly depends on interface states density and capture probability. As the interface defect density is nearly identical for all iron contamination doses, we still observe a decrease of PL signal with increased contamination, but with a lower sensitivity to volume contamination as the variations are more restrained with only a 30% drop for the most contaminated sample compared to the reference.

In inversion, surface is passivated with a symmetrical process compared to accumulation, as the holes diffuse to the volume and recombine less actively with interface defects. The sensitivity to iron defect states is increased again but not as much as in accumulation. This difference resides in the dissymmetry of hole and electron capture cross section in Si.

3.2.2. Copper

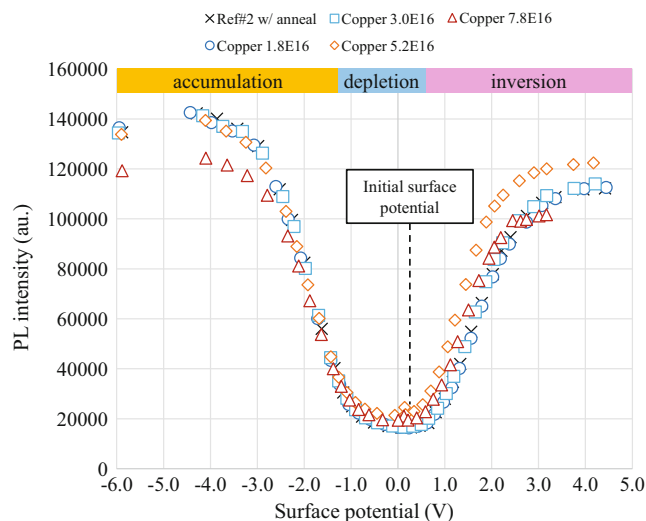**Figure 8** shows the PL–V curves obtained for the copper contaminated samples. The PL–V variations between wafers are less important than for iron but, opposite to the iron samples, copper surface contamination only varies in one order of magnitude from the less to the most contaminated sample. In deep accumulation, the PL intensity of all wafers is very close to the reference sample, except for the most contaminated wafer whose PL intensity is around 10% lower. As for the iron contaminated samples, copper wafers were all initially positioned in depletion, thus the variation observed are the same as the variations in Figure 6. In strong inversion, the most contaminated wafer displays again the lowest PL intensity, while the second most contaminated remains with the highest signal.

The observed behavior can be explained in the same way as the iron in accumulation, depletion, and inversion. The main difference consists in the interface defect density that varies with the contamination dose.

In depletion, the PL signal is consistent with measured interface defect density. The sensitivity to copper contamination is improved in an indirect way because of the D_{it} reduction due to the supposed behavior of copper atoms at the interface, discussed in Section 3.1. This D_{it} decrease has impact on PL until inversion regime, where the most contaminated sample shows the lowest PL intensity, since corona charges increases again the surface electric field and reduces surface recombinations. As explained for the iron contaminated wafers, the dissymmetry of the electrons and holes capture cross section in Si reduces the surface passivation efficiency in the inversion regime. Therefore, the copper sample with the lowest D_{it} still shows the highest PL signal.

3.2.3. Summary of PL–V Measurements

In accumulation, metallic contamination generally reduces the PL signal by introducing additional electrically active energy levels in the Si bandgap. In depletion, not only PL is sensitive to metallic contamination, but also to surface recombination due to poor interface passivation. Thus, metallic contamination cannot always be directly associated to a PL intensity decrease

as showed with copper. By leading the characterized samples into accumulation or inversion, surface recombination are reduced and the sensitivity of PL measurement to metallic contamination can be highly improved as showed with iron. Corona discharge is invasive, consequently it is not compatible with production wafers. However, the method presented could bring added values for troubleshooting during contamination events.

In the point of view of in-line detection of contamination on full wafers, surface passivation is rarely homogeneous. Therefore, MacroPL could be used to detect contamination taking the form of small, localized areas of unusual PL intensity. For example, brighter areas could be associated to copper or other metals that share the same enhancement properties, while darker areas could be associated to most of the other transition metals. Figure 5a shows a good example for iron detection on clean substrate. Finally, in the same manner as SPV, we can also imagine using PL before and after iron boron pairs activation to differentiate iron among all the possible transition metals.[21]

4. Conclusion

Room temperature macroscopic PL and PLS has been performed on low level copper and iron contaminated samples. Combined with corona discharges and surface potential measurements, bias dependent PL has been acquired to separate contamination effects on PL signal from surface recombination variations due to different interface quality. Copper contamination has been shown to interact with interface defects and enhance the PL signal at low contamination. It is only by increasing further the contamination that the impact of copper electrical active centers becomes predominant on the PL signal. The sensitivity of PL to iron has also been acknowledged for all band regimes. We showed an enhancement of sensitivity with better surface passivation when reducing surface recombination. Therefore, this study showed the importance of surface properties control to correctly understand the PL signal and is a valuable input for industrial in-line adoption of PL for metallic contamination detection.

Conflict of Interest

The authors declare no conflict of interest.

Data Availability Statement

The data that support the findings of this study are available from the corresponding author upon reasonable request.

[1] M. L. Polignano, G. Borionetti, A. Galbiati, S. Grasso, I. Mica, A. Nutsch, *Spectrochim. Acta, Part B* **2018**, *149*, 313.
[2] K. Graff, *Metal Impurities in Silicon-Device Fabrication*, 2nd ed., vol. 24, Springer-Verlag Berlin Heidelberg, Berlin **2000**.
[3] L. Fabry, L. Koster, S. Pahlke, L. Kotz, J. Hage, *IEEE Trans. Semicond. Manuf.* **1996**, *9*, 428.
[4] A. Danel, U. Staube, G. Kamarinos, E. Kamieniecki, F. Tardif, *The Electrochemical Society* (Ed.: J. Ruzyllo, R. E. Novak), Electrochemical Society, Pennington, NJ, **1998**, pp. 400-407.
[5] D. Shindo, T. Oikawa, *Analytical Electron Microscopy for Materials Science*, Springer Japan, Tokyo **2002**.
[6] D. Hellin, S. De Gendt, J. Rip, C. Vinckier, *IEEE Trans. Device Mater. Reliab.* **2005**, *5*, 639.
[7] A. M. Goodman, *J. Appl. Phys.* **1961**, *32*, 2550.
[8] H. De Witte, S. De Gendt, M. Douglas, T. Conard, K. Kenis, P. W. Mertens, W. Vandervorst, R. Gijbels, *J. Electrochem. Soc.* **2000**, *147*, 1915.
[9] M. Horn, *Fresenius' J. Anal. Chem.* **1999**, *364*, 385.
[10] M. L. Polignano, A. Galbiati, I. Mica, D. Magni, D. Cseh, F. Jay, P. Basa, N. Laurent, I. Lajtos, G. Molnar, L. Dudas, L. Roszol, L. Jastrzebski, *ECS J. Solid State Sci. Technol.* **2018**, *7*, R12.
[11] S.-K. J. Jian, C.-C. Jeng, W. S. Yoo, *AIP Adv.* **2012**, *2*, 042164.
[12] V. Higgs, F. Chin, X. Wang, *Electrochemical Society Proceedings*, vol. 99–16, The Electrochemical Society, Pennington, NJ **1999**, p. 21.
[13] T. Gfroerer, *Encyclopedia of Analytical Chemistry*, John Wiley & Sons, **2006**, pp. 9209–9231 https://doi.org/10.1002/9780470027318.a2510.
[14] T. Nassiet, R. Duru, D. Le-Cunff, A. Arnaud, J. Bluet, G. Bremond, in *2020 31St Annual SEMI Advanced Semiconductor Manufacturing Conference (ASMC)*, IEEE, **2020**, pp. 1-6 https://doi.org/10.1109/ASMC49169.2020.9185305.
[15] W. D. Scott, A. Stevenson, *J. Electrochem. Soc.* **2004**, *151*, G8.
[16] A. Haug, *Phys. Status Solidi (B)* **1981**, *108*, 443.
[17] J. Lagowski, P. Edelman, A. M. Kontkiewicz, O. Milic, W. Henley, M. Dexter, L. Jastrzebski, A. M. Hoff, *Appl. Phys. Lett.* **1993**, *63*, 3043.
[18] M. Wilson, J. Lagowski, A. Savtchouk, L. Jastrzebski, J. 'Amico, *Gate Dielectric Integrity: Material, Process, and Tool Qualification* (Eds.: D. Gupta, G. Brown), ASTM International, West Conshohocken, PA **2000**, pp. 74-90.
[19] M. Nakamura, S. Murakami, *Jpn. J. Appl. Phys.* **2010**, *49*, 071302.
[20] H. Haug, Ø. Nordseth, E. V. Monakhov, E. S. Marstein, *Sol. Energy Mater. Solar Cells* **2012**, *106*, 60.
[21] D. Macdonald, J. Tan, T. Trupke, *J. Appl. Phys.* **2008**, *103*, 073710.